European Radiology (2019) 29:251–258
https://doi.org/10.1007/s00330-018-5569-x

CARDIAC

3D-printed heart model to guide LAA closure: useful in clinical practice?

Anne-Lise Hachulla[1] · Stéphane Noble[2] · Gabriel Guglielmi[1] · Daniel Agulleiro[3] · Hajo Müller[2] · Jean-Paul Vallée[1]

Received: 12 February 2018 / Revised: 19 April 2018 / Accepted: 28 May 2018 / Published online: 14 June 2018

Abstract

Objectives Correct device sizing for left atrial appendage (LAA) closure remains challenging due to complex LAA shapes. The aim of our study was to investigative the utility of personalized 3D-printed models (P3DPM) of the LAA to guide device size selection.

Methods Fifteen patients (75.4 ±8.5years) scheduled for LAA closure using an Amulet device underwent cardiac computed tomography (CT). The LAA was segmented by semiautomatic algorithms using Vitrea® software. A 1.5-mm LAA thick shell was exported in stereolithography format and printed using TangoPlus flexible material. Different Amulet device sizes on the P3DPM were tested. New P3DPM-CT with the device was acquired in order to appreciate the proximal disc sealing the LAA ostium and the compression of the distal lobe within the LAA. We predicted the device size with P3DPM and compared this with the device sizes predicted by transesophageal echocardiography (TEE) and CT as well as the device size implanted in patients.

Results The device size predicted by 3D-TEE and CT corresponded to the implanted device size in 8/15 (53%) and 10/15 (67%), respectively. The predicted device size from the P3DPM was accurate in all patients, obtaining perfect contact with the LAA wall, without device instability or excessive compression. P3DPM-CT with the deployed device showed device deformation and positioning of the disk in relation to the pulmonary veins, allowing us to determine the best device size in all 15 cases.

Conclusion P3DPM allowed us to simulate the LAA closure procedure and thus helped to identify the best Amulet size and position within the LAA.

Key Points

- *A 3D-printed heart model allows to simulate the LAA closure procedure.*
- *A 3D-printed heart model allowed to identify the optimal Amulet size and position.*
- *3D-printed heart models may contribute to reduce the Amulet implantation learning curve.*

Keywords Atrial appendage · Atrial fibrillation · 3D printing · Personalized 3D-printed models · New emerging technology

Anne-Lise Hachulla and Stéphane Noble contributed equally to this work.

Electronic supplementary material The online version of this article (https://doi.org/10.1007/s00330-018-5569-x) contains supplementary material, which is available to authorized users.

✉ Anne-Lise Hachulla
anne-lise.hachullalemaire@hcuge.ch

[1] Division of Radiology, University Hospitals of Geneva, Rue Gabrielle-Perret-Gentil 4, 1291 Geneva, Switzerland

[2] Department of Cardiology, University Hospitals of Geneva, Geneva, Switzerland

[3] Computer Science Center, Faculty of Science, Carouge, Switzerland

Abbreviations

2D	2-dimensional
3D	3-dimensional
CT	Computed tomography
LAA	Left atrial appendage
P3DPM	Personalized 3D-printed model
STL	Stereolithography
TEE	Transesophageal echocardiography

Introduction

In patients with atrial fibrillation (AF), the risk of stroke is increased by 4 to 5 times and it has been demonstrated that 90% of left atrial thrombi are localized in the left atrial

appendage (LAA) [1]. In this context, percutaneous LAA closure devices have been developed over the last 15 years. Currently, most of the reported data comes from experience with the two most used devices available in Europe, namely the Food and Drug Administration (FDA)-approved Watchman device (Boston Scientifics) and the Amplatzer cardiac plug (ACP) device and its next generation, the Amulet (Abbott Vascular).

The correct sizing and the optimal implantation position of the closure device remain challenging due to complex and variable LAA shapes (i.e. cactus, cauliflower, chicken wing and windsock) [2]. Several imaging techniques [i.e. fluoroscopy, 2-dimensional (2D) or 3-dimensional (3D) transesophageal echocardiography (TEE), intra-cardiac echocardiography (ICE) and cardiac computed tomography (CT) scan] are available to measure the landing zone and select the correct device size [3]. The vast majority of procedures are performed under TEE or even ICE guidance. However, a mean of 1.8 devices were required to perform the procedure in PROTECT AF [4].

The aim of our study was to investigative the utility of personalized 3D-printed heart models of the LAA created from cardiac CT to facilitate device size selection and identify the best position within the LAA.

Materials and methods

Patient selection and standard imaging analysis

Fifteen consecutive patients (mean age 75.4 ±8.5 years, 60% male) scheduled for LAA closure were included in our series between January 2016 and April 2017. All patients had persistent or permanent atrial fibrillation, ischemic cerebrovascular events and contraindication for anticoagulation. All procedures were performed under general anaesthesia with 3D-TEE and fluoroscopic guidance. When TEE was not performed before the day of the intervention, TEE measurements with 3D reconstructions were done under general anaesthesia before the venous puncture. In a formal pre-procedural consultation with the operator, all patients were fully informed about the procedural risks before providing informed consent for the procedure. The local institutional review board approved the study (number: 2017-01969).

As a pre-procedural assessment, all underwent a cardiac CT scan with 80 mL of contrast media injection at a flow rate of 4 mL/s. (400 mg I/mL, iomeprol, Bracco). All examinations were performed on a second-generation, dual-source, 128-slice multidetector CT (MDCT) system (Somatom Definition Flash, Siemens Healthineers). The prospective flash ECG-gated cardiac CT acquisition was performed using the following parameters: pitch = 3.4; rotation time: 0.28s; collimation: 64 x 2 x 0.6 mm and synchronized to atrial diastole, corresponding to a ventricular systole (30% of the R-R interval). A late enhanced CT at 70 seconds was completed in cases where full contrast enhancement of the LAA was not achieved. Image data was then reconstructed using iterative algorithms (ADMIRE®-strength 3-kernel I26f) with a section thickness/increment of 0.6/0.3 mm.

We measured the mean diameter and the derived diameter from the perimeter measured manually on the 3D reconstructions of the landing zone—defined as the maximal LAA diameter at 10 mm inside the LAA—and of the LAA ostium. Considering the 3D-TEE and CT scan measurements, the device was selected according to the manufacturer's chart.

3D-printed model

The left atrium without the interatrial septum was segmented by semiautomatic algorithms using Vitrea® software (Vital Images, Inc.). A 1.5-mm-thick shell of the LAA was created in order to have a flexible but resistant material allowing a deformation of the device without breaking the model; it was exported in stereolithography (STL) format and finally printed on an Objet260 Connex3 printer (Stratasys Ltd.) using TangoPlus FLX 930 flexible material. The different LAA shapes were classified as cauliflower, chicken wing, cactus or windsock (Fig. 1).

Several sizes of Amulet cardiac plug devices were deployed into the 3D-printed model. Furthermore, once the device size was selected, different device positions were tested (i.e. deep deployment in a lobe or more proximal deployment), representing a simulation of the LAA procedure. The criteria used to predict the device size by the 3D-printed models were:

- The presence of a device-lobe compression assessed visually when only the lobe was deployed without device luxation,
- The stability of the device lobe while pulling on it with controlled force,
- Complete sealing of the LAA ostium by the device disk,
- Absence of overlap of the pulmonary vein ostia by the device disk.

Finally, a new CT scan of the 3D-printed model with and without the device inside the LAA was performed using the selected device size in order to confirm that all criteria of the best device size were met. Furthermore, the mean landing zone diameter and the device compression of the 3D-printed model were calculated with and without the device inside in order to evaluate the potential deformation of the 3D-printed model generated by the device [5].

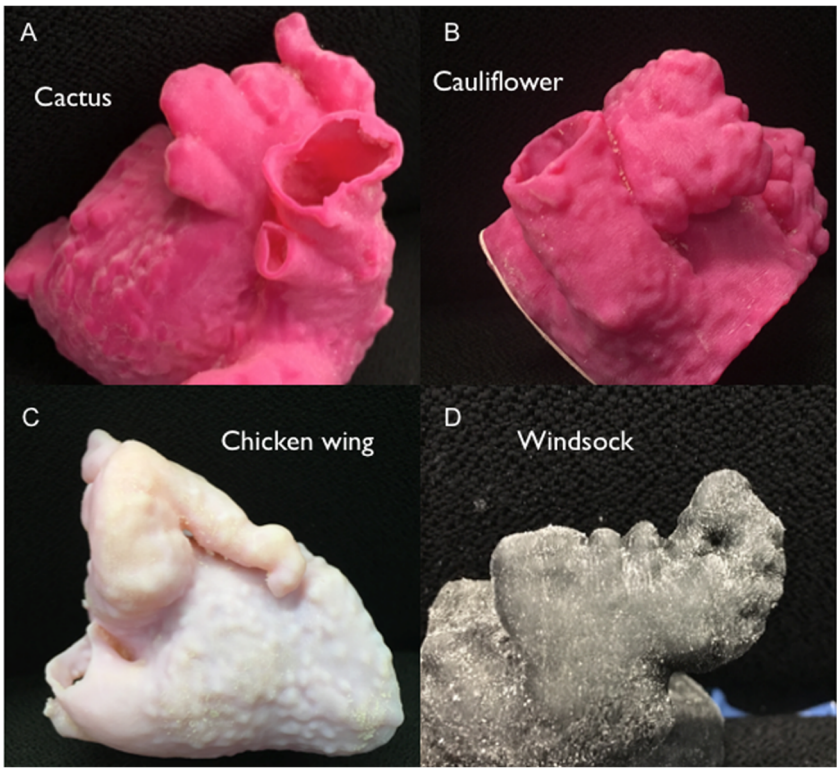

Fig. 1 Different LAA shapes. **A** cactus, **B** cauliflower, **C**. chicken wing and **D** windsock

Percutaneous LAA closure procedure and follow-up

The patients underwent percutaneous LAA closure with the Amulet device. Patients were hydrated to achieve an LA pressure > 12 mmHg after the trans-septal puncture. The size of the device implanted in the patient was recorded and compared to the predicted sizes by TEE, cardiac CT and the 3D-printed model. CT-, TEE- and 3D-printed model-based prediction were validated against the final implant size.

At the end of the procedure, TEE and fluoroscopic assessment of residual filling of the LAA were performed and the pericardium space was assessed in order to exclude the presence or the worsening of a prior pericardial effusion. According to our institutional protocol, all patients underwent chest X-ray and a transthoracic echocardiogram at day 1.

Complications such as device embolization, cardiac tamponade, stroke and mortality were assessed at discharge. As part of our protocol, patients are routinely followed up to 6 months with a TEE scheduled between 4- to 6-month post-procedure. When a control TEE cannot be performed (e.g. patient refuses or major discomfort requiring general anaesthesia), a CT scan is scheduled.

Statistical analysis

Categorical data are presented as numbers and percentages, whereas continuous data are expressed as mean ± standard deviation (SD) or median (interquartile range) according to their distribution. Normal distribution of the data was assessed through a Kolmogorov–Smirnov test and a Shapiro–Wilk test. Pearson correlation was used to compared device sizes predicted by TEE, CT, the 3D-printed heart model and the implanted device size. All analyses were performed using the Statistical Package for the Social Sciences (SPSS) software (version 20.0, SPSS Inc., Chicago, IL, USA).

Results

Patient and 3D-printed heart model characteristics

LAA shapes observed were cactus in 6 patients (40%), cauliflower in 2 (13%), chicken wing in 4 (27%) and windsock in 3 (20%).

CT data (mean effective dose: 1.21 ±0.85 mSv) from all the 15 patients were easily and successfully segmented. The segmentation process to export an STL format lasted less than 15 min for all cases and the mean time for printing the model was approximately 8 hours. The mean price was Swiss Franc (CHF) 235.7 ± 79.8 for the 3D-printed heart model and CHF 6,500 for one Amulet device.

Procedural characteristics and results

Success of device implantation was achieved in all procedures with no stroke, mortality, device embolization or cardiac

tamponade at discharge. The median number of devices used during the procedure was 1 (1–3).

Predicted device size by TEE, CT and 3D-printed models vs. implanted device size

A poor correlation of mean LAA diameters was found between TEE and CT. Mean diameters were lower with TEE (18.9 ±2.8 mm) than with CT (20.4 ±2.7mm; Pearson correlation coefficient r = 0.53; R squared = 0.28; $p = 0.04$). The device size predicted by TEE and CT corresponded to the implanted device size in 8/15 (53% Pearson correlation coefficient r = 0.79; R squared = 0.63; $p < 0.001$) and 10/15 (67%; Pearson correlation coefficient r = 0.89; R squared = 0.79; $p < 0.001$), respectively. The predicted device size based on the 3D-printed model was accurate in all 15 patients (100%; Pearson correlation coefficient r = 1; R squared = 1; $p < 0.001$; Figs. 2 and 3).

On the 3D-printed model, device compression within the LAA wall and the proximal disc sealing the LAA ostium were easily confirmed in all 15 cases. In cases of incorrect sizing, the absence of device compression, device instability or excessive device compression were easily visually identified.

CT scan of the 3D-printed model with the deployed device showed device deformation and positioning of the disk in relation to the pulmonary veins, allowing us to determine the best device size in all 15 cases. The five cases where device size was falsely predicted by CT were related to instability of the device (n = 2), incomplete sealing of the LAA ostium (n = 2) and overlap of the pulmonary vein ostia (n = 1; Fig. 4).

Furthermore, the mean landing zone diameter of the LAA was significantly greater with the device inside the LAA (19.9 ±2.2 mm vs. 21.6 ±2.9 mm; $p = 0.0003$; without and with the device, respectively), corresponding to an increase of 7.9%; and the mean ostium diameter of the LAA was significantly greater with the device ($p < 0.0001$; 24.2 ±2.7 mm vs. 26.7 ±2.6 mm; $p < 0.0001$, without and with the device, respectively) corresponding to an increase of 9.3%. The 3D-printed model was significantly deformed according to CT scan assessment with and without a deployed device in the model with a mean percentage of compression of 11.3 ± 6.2%. The device deformation was also visually identified (Fig. 5).

Discussion

As the main finding of our study, the personalized 3D-printed model allowed us to predict the Amulet device size in all 15 patients and outperform the predictions based either on CT alone or TEE. In addition, we showed that the 3D-printed model using flexible material with a 1.5-mm-thick shell was significantly deformed according to CT scan assessment with and without a deployed device in the model (11.3 ± 6.2% difference).

LAA is a complex multiform structure. The morphology, diameter, depth, and lobulation of the LAA add difficulty to estimate the device size and positioning. These many variables need to be carefully considered to select the correct device size. The risks of under- or oversizing are LAA perforation, pericardial effusion, interference with the mitral valve or the ostium of the pulmonary veins, compression of the left circumflex artery and device embolization [6].

As recently emphasized by a consensus document [7] in agreement with a survey in 33 European medical centers [8], 2D-TEE is the method of choice for LAA anatomical assessment to select the closure device size. However, several studies have consistently demonstrated that 2D-TEE underestimates the diameter of the LAA compared to cardiac CT [9–13] and our findings are in agreement with these results.

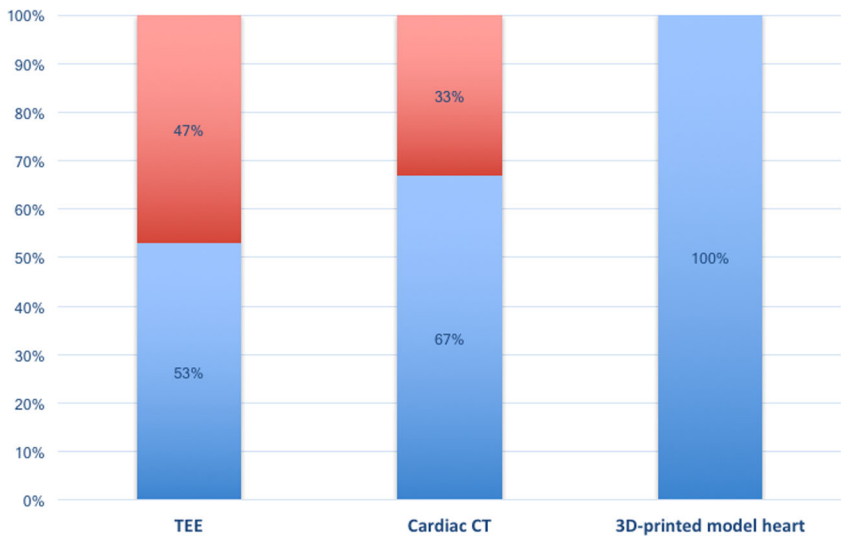

Fig. 2 Device size prediction by the different image modalities The device size predicted by TEE and cardiac CT corresponded to the implanted device size in 8/15 (53%) and 10/15 (67%), respectively. The predicted device size based on the 3D-printed heart model was accurate in all 15 patients without circumferential leakage nor adverse events after the procedure. (in blue: correct prediction; in red: wrong prediction)

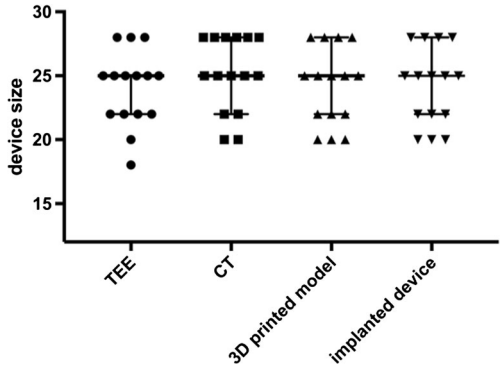

Fig. 3 Correlation between device sizes predicted by TEE, CT, 3D-printed heart model and the finally implanted device size

The origin of the discrepancy between cardiac CT and 2D-TEE may be related to the difficulty in defining the optimal alignment plane in 2D-TEE as proposed by Budge et al. since they also observed a trend in underestimating LAA diameter when using only 2D planar CT images [9]. With respect to 3D-TEE, contradictory results emerged with more than 50% of incorrect Watchman size prediction using 3D-TEE [13], but an almost perfect match between CT and 3D-TEE in other series [12, 14]. Another explanation for the difference between CT and TEE measurements may be related to the loading condition and LA pressure—generally decreased in general anaesthesia—that influence LAA volume [15]. However, Wang et al. showed that despite LA mean pressure > 10 mmHg, 2D- and 3D-TEE still undersize LAA measurement compared to CT scanning [13].

The difference in LAA diameter measurements between CT and 2D-TEE should support the use of the 3D assessment provided by CT scan or 3D-TEE in pre-procedural planning of LAA closure. However, the official instructions for use for both the Watchman and Amulet devices consider the 2D-TEE maximal diameter as the reference measurement despite the limitations related to the commonly oval shape of the LAA at the landing zone. Indeed, Al-Kassou et al. showed that the 3D-TEE-derived diameter from the perimeter of the landing zone is the most accurate parameter for determining the optimal device size [5].

Despite the results of the randomized PROTECT AF trial (the WATCHMAN LAA System for Embolic Protection in Patients with Atrial Fibrillation) showing non-inferiority of the device to warfarin for the primary end point, safety concerns were raised [16]. Indeed, 7.7% of the patients presented procedure/device-related adverse events within 7 days (4.1% serious pericardial effusion, 0.5% procedural stroke, 0.6% device embolization and 3.5% major bleeding), partially related to the learning curve as suggested by the reduction of these complications in the second part of the study and in the subsequent studies [16–18]. LAA closure is now considered a valid alternative to anticoagulation for patients at high risk

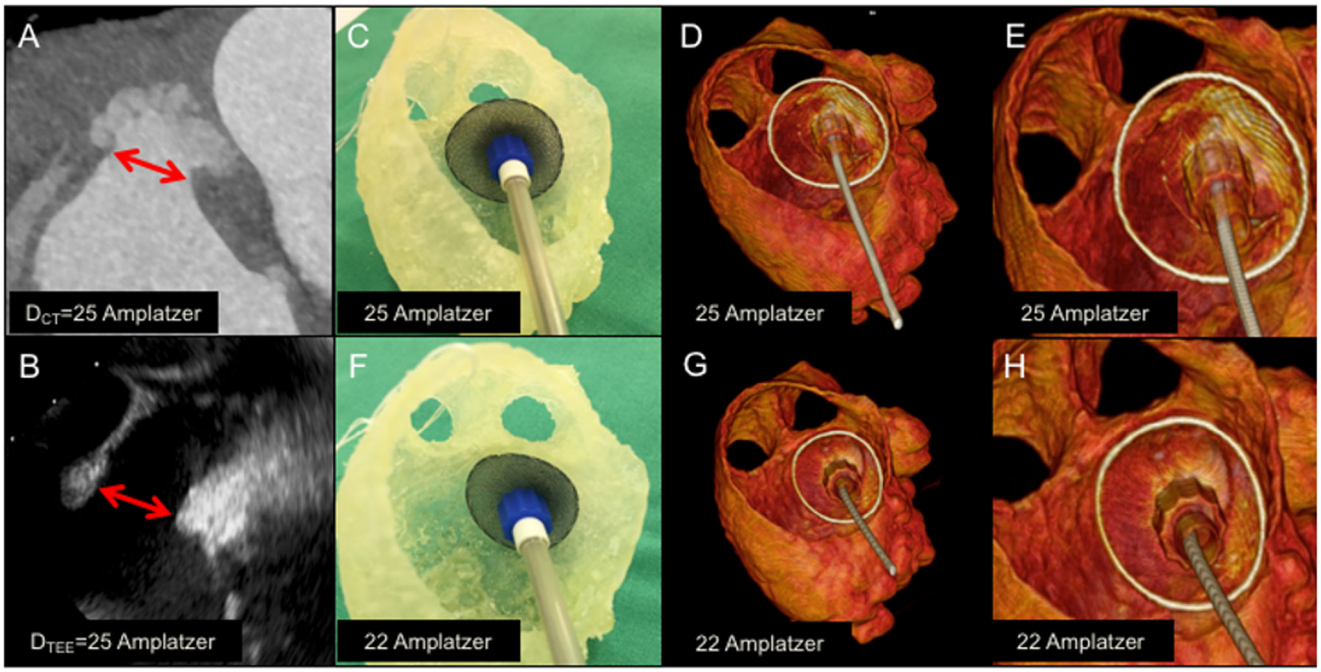

Fig. 4 Example of a cauliflower LAA in an 84-year-old man. Both cardiac CT (**A**) and TEE (**B**) predicted a 25-mm Amulet device. Two different Amulet sizes were tested: 25 mm (**C**) and 22 mm (**F**). Thanks to the 3D-printed model, we can observe that the disc of the 25-mm Amulet device was too large and that it partially covered the ostium of the pulmonary vein. This was confirmed by the CT of the 3D-printed model (**D**–**E**). On the other hand, the disc of the 22-mm Amulet device perfectly sealed the ostium without interfering with the pulmonary veins. This was confirmed by the CT of the 3D-printed model (**G**–**H**). The procedure was successfully performed with a 22-mm Amulet device as predicted with the 3D-printed model

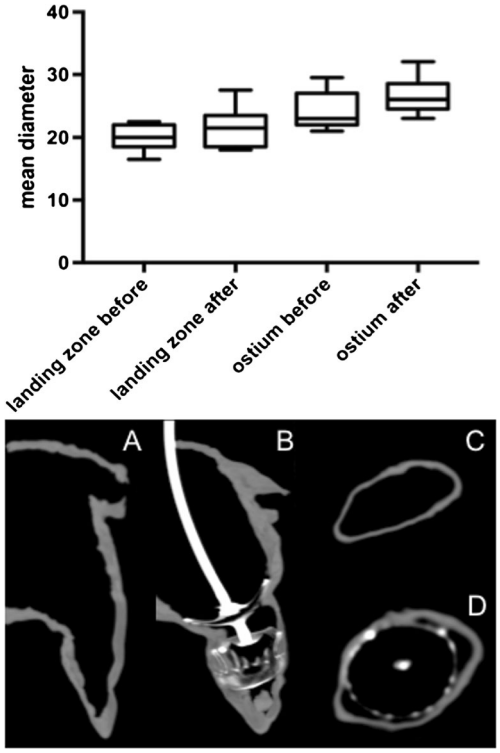

Fig. 5 Measurements of the 3D-printed heart model with and without deployed device. The mean landing zone diameter and mean ostium diameter were significantly greater with the deployed device (p = 0.0003 and $p < 0.0001$, respectively; upper panel). The increased size of the LAA and the deformation of the device were clearly analysed using the CT of the 3D-printed model with (**B**/**D**) and without (**A**/**C**) the device inside the 3D-printed heart model (lower panel)

of bleeding or with a contraindication to anticoagulation and thus an increasing number of operators are embracing the technique. Therefore, strategies to accelerate the learning curve and facilitate procedure planning—by understanding the specific anatomy of the patient and helping the device sizing and placement—are welcomed.

The rapid development of 3D-printed heart models is particularly pertinent to LAA closure since even when using advanced imaging methods, it is difficult to assess its anatomy (variable shape) and predict the interaction between the device and LAA. To date, several case reports or series of 3D-printed model use—mainly in cases of Watchman implantations—showed accurate sizing and an optimal implanted device [11, 13, 19–24]. Interestingly, the use of 3D-printed models in a prospective randomized trial of 42 patients by Li et al. showed a significant reduction of the radiation time in the group with 3D-printed models compared to the group using TEE [23]. Less information regarding the Amulet device is available. Bieliauskas et al. confirmed in a preliminary report that the use of 3D-printed models could reduce the number of devices used per procedure, procedural time and contrast use compared with historical data with TEE and CT only [21].

Our study of 15 patients with Amulet implantation demonstrated that 3D-printed models provide an accurate estimate of LAA size and anatomy compared to standard imaging and can help in device positioning. While silicone rubber may not precisely mimic the elasticity and distensibility of the human LAA, scanning of our models with a deployed Amulet device showed device compression and 3D-printed LAA deformation. In our study, CT scan assessment with a deployed device in the model was useful to better understand the device implantation after a "virtual" procedure in order to improve the learning curve and to facilitate the true procedure. The only report of scanning the 3D-printed model with a deployed device was with the Watchman device and showed that the device compression in patients corresponded well with the predicted compression in the 3D-printed model [11].

Our study has several limitations. It is a single-center study only focusing on the Amulet device with a limited number of patients. Other studies involving 3D-printed models have shown accurate size prediction for the Watchman device [11, 23, 24] except one [22]. In our study, the device size and position were not assessed at the end of the procedure by a CT but by TEE and fluoroscopy. Our series and the current literature are an incentive to perform a large study to confirm the benefit of this strategy. A complete cost-benefit study has not been performed. Considering that the price of a 3D print is approximately 3% of the price of a device in our country, the extra cost related to the 3D-printed model seems acceptable, especially if we can decrease associated complications. The 3D-printed heart model created from CT data has some limitations with respect to the amount of contrast media required and the X-ray exposure, whereas 3D-printed heart models can also be created from 3D-TEE with good clinical results [25]. However, the latter still needs to be improved as results at cardiac CT follow-up were sub-optimal since persistent LAA contrast filling was observed in 62% of the patients post-procedure [25].

Although, the TangoPlus material is flexible and demonstrated deformation after insertion of the device, we did not evaluate the difference of elasticity of our 3D-printed heart model with the LAA wall. More work is needed in this field, as it is possible to vary the degree of stiffness of the 3D models. However, our current set-up was already able to reliably predict the correct device size. We did not include the interatrial septum in our model. Additional information may potentially be obtained if the atrial septum is included in the model, in order to assess the best area for the trans-septal puncture and which delivery system to use, especially concerning the Watchman device. Finally, the dimensions of the landing zone are dependent on the loading conditions and increase after systematic volume loading. However, CT scan measures were performed without intravenous pre-hydration or knowledge of the LA pressure.

In conclusion, among a consecutive series of 15 patients, a personalized 3D-printed heart model allowed us to simulate the LAA closure procedure and thus helped to identify the best Amulet size and position within the LAA. The use of 3D-printed heart models may contribute to reduce the Amulet implantation learning curve. Further large prospective multicentric studies are required to confirm these benefits.

Acknowledgements This work was presented at the last TCT meeting in Denver.

Funding GEcor Fondation (foundation for cardiology research at the cardiology division at the University Hospital of Geneva). Some of the devices were provided by St. Jude Medical; some were recuperated after a mis-sizing

Compliance with ethical standards

Guarantor The scientific guarantor of this publication is Jean-Paul Vallée.

Conflict of interest The authors of this manuscript declare no relationships with any companies, whose products or services may be related to the subject matter of the article.

Statistics and biometry No complex statistical methods were necessary for this paper.

Informed consent Written informed consent was obtained from all subjects (patients) in this study.

Ethical approval Institutional review board approval was obtained.

Methodology
- retrospective
- diagnostic or prognostic study
- performed at one institution

References

1. Blackshear JL, Odell J (1996) Appendage obliteration to reduce stroke in cardiac surgical patients with atrial fibrillation. Ann Thorac Surg 61:755–759
2. Saw J, Lopes JP, Reisman M, McLaughlin P, Nicolau S, Bezerra HG (2016) Cardiac computed tomography angiography for left atrial appendage closure. Can J Cardiol 32(1033):e1031–e1039
3. Matsuo Y, Neuzil P, Petru J et al (2016) Left atrial appendage closure under intracardiac echocardiographic guidance: feasibility and comparison with transesophageal echocardiography. J Am Heart Assoc 5(10). https://doi.org/10.1161/JAHA.116.003695
4. Reddy VY, Doshi SK, Sievert H et al (2013) Percutaneous left atrial appendage closure for stroke prophylaxis in patients with atrial fibrillation: 2.3-year follow-up of the PROTECT AF (Watchman Left Atrial Appendage System for Embolic Protection in Patients with Atrial Fibrillation) Trial. Circulation 127:720–729
5. Al-Kassou B, Tzikas A, Stock F, Neikes F, Volz A, Omran H (2017) A comparison of two-dimensional and real-time 3D transoesophageal echocardiography and angiography for assessing the left atrial appendage anatomy for sizing a left atrial appendage occlusion system: impact of volume loading. EuroIntervention 12:2083–2091
6. Park JW, Bethencourt A, Sievert H et al (2011) Left atrial appendage closure with Amplatzer cardiac plug in atrial fibrillation: initial European experience. Catheter Cardiovasc Interv 77:700–706
7. Casu G, Gulizia MM, Molon G et al (2017) ANMCO/AIAC/SICI-GISE/SIC/SICCH Consensus Document: percutaneous occlusion of the left atrial appendage in non-valvular atrial fibrillation patients: indications, patient selection, staff skills, organisation, and training. Eur Heart J Suppl 19:D333–D353
8. Pison L, Potpara TS, Chen J et al (2015) Left atrial appendage closure-indications, techniques, and outcomes: results of the European Heart Rhythm Association Survey. Europace 17:642–646
9. Budge LP, Shaffer KM, Moorman JR, Lake DE, Ferguson JD, Mangrum JM (2008) Analysis of in vivo left atrial appendage morphology in patients with atrial fibrillation: a direct comparison of transesophageal echocardiography, planar cardiac CT, and segmented three-dimensional cardiac CT. J Interv Card Electrophysiol 23:87–93
10. Chow DH, Bieliauskas G, Sawaya FJ et al (2017) A comparative study of different imaging modalities for successful percutaneous left atrial appendage closure. Open Heart 4:e000627
11. Hell MM, Achenbach S, Yoo IS et al (2017) 3D printing for sizing left atrial appendage closure device: head-to-head comparison with computed tomography and transesophageal echocardiography. EuroIntervention. https://doi.org/10.4244/EIJ-D-17-00359
12. Nucifora G, Faletra FF, Regoli F et al (2011) Evaluation of the left atrial appendage with real-time 3-dimensional transesophageal echocardiography: implications for catheter-based left atrial appendage closure. Circ Cardiovasc Imaging 4:514–523
13. Wang DD, Eng M, Kupsky D et al (2016) Application of 3-dimensional computed tomographic image guidance to WATCHMAN implantation and impact on early operator learning curve: single-center experience. JACC Cardiovasc Interv 9:2329–2340
14. Yosefy C, Azhibekov Y, Brodkin B, Khalameizer V, Katz A, Laish-Farkash A (2016) Rotational method simplifies 3-dimensional measurement of left atrial appendage dimensions during transesophageal echocardiography. Cardiovasc Ultrasound 14:36
15. Spencer RJ, DeJong P, Fahmy P et al (2015) Changes in left atrial appendage dimensions following volume loading during percutaneous left atrial appendage closure. J Am Coll Cardiol Intv 8:1935–1941
16. Holmes DR, Reddy VY, Turi ZG et al (2009) Percutaneous closure of the left atrial appendage versus warfarin therapy for prevention of stroke in patients with atrial fibrillation: a randomised non-inferiority trial. Lancet 374:534–542
17. Holmes DR Jr, Kar S, Price MJ et al (2014) Prospective randomized evaluation of the Watchman Left Atrial Appendage Closure device in patients with atrial fibrillation versus long-term warfarin therapy: the PREVAIL trial. J Am Coll Cardiol 64:1–12
18. Reddy VY, Holmes D, Doshi SK, Neuzil P, Kar S (2011) Safety of percutaneous left atrial appendage closure: results from the Watchman Left Atrial Appendage System for Embolic Protection in Patients with AF (PROTECT AF) clinical trial and the Continued Access Registry. Circulation 123:417–424
19. Otton JM, Spina R, Sulas R et al (2015) Left atrial appendage closure guided by personalized 3D-printed cardiac reconstruction. JACC Cardiovasc Interv 8:1004–1006
20. Obasare E, Melendres E, Morris DL, Mainigi SK, Pressman GS (2016) Patient specific 3D print of left atrial appendage for closure device. Int J Card Imaging 32:1495–1497
21. Bieliauskas G, Otton J, Chow DHF et al (2017) Use of 3-dimensional models to optimize pre-procedural planning of

percutaneous left atrial appendage closure. JACC Cardiovasc Interv 10:1067–1070
22. Goitein O, Fink N, Guetta V et al (2017) Printed MDCT 3D models for prediction of left atrial appendage (LAA) occluder device size: a feasibility study. EuroIntervention 13:e1076–e1079
23. Li H, Qingyao B et al (2017) Application of 3D printing technology to left atrial appendage occlusion. Int J Cardiol 231:258–263
24. Vaquerizo B, Escabias C, Dubois D, Gomez G, Barreiro-Perez M, Cruz-Gonzalez I (2017) Patient-specific 3D-printed cardiac model for percutaneous left atrial appendage occlusion. Rev Esp Cardiol. https://doi.org/10.1016/j.rec.2017.05.028
25. Liu P, Liu R, Zhang Y, Liu Y, Tang X, Cheng Y (2016) The value of 3D printing models of left atrial appendage using real-time 3D transesophageal echocardiographic data in left atrial appendage occlusion: applications toward an era of truly personalized medicine. Cardiology 135:255–261